BBA - Biomembranes 1865 (2023) 184217

Contents lists available at ScienceDirect

BBA - Biomembranes

journal homepage: www.elsevier.com/locate/bbamem

Identification of membrane engineering targets for increased butanol tolerance in *Clostridium saccharoperbutylacetonicum*

John A. Linney [a], Sarah J. Routledge [a], Simon D. Connell [b], Tony R. Larson [c], Andrew R. Pitt [d], Elizabeth R. Jenkinson [e], Alan D. Goddard [a,*]

[a] School of Health and Life Sciences, Aston University, Aston Triangle, Birmingham B4 7ET, UK
[b] School of Physics and Astronomy and The Astbury Centre for Structural Molecular Biology, University of Leeds, Leeds LS2 9JT, UK
[c] Department of Biology, University of York, York YO10 5DD, UK
[d] Manchester Institute of Biotechnology, University of Manchester, Manchester M1 7DN, UK
[e] Biocleave, 154AH Brook Drive, Milton Park, Abingdon, Oxfordshire OX14 4SD, UK

ARTICLE INFO

Keywords:
Butanol toxicity
Lipid membrane
Lipidomics
Clostridia
In vitro stability assays
Atomic force microscopy

ABSTRACT

There is a growing interest in the use of microbial cell factories to produce butanol, an industrial solvent and platform chemical. Biobutanol can also be used as a biofuel and represents a cleaner and more sustainable alternative to the use of conventional fossil fuels. Solventogenic Clostridia are the most popular microorganisms used due to the native expression of butanol synthesis pathways. A major drawback to the wide scale implementation and development of these technologies is the toxicity of butanol. Various membrane properties and related functions are perturbed by the interaction of butanol with the cell membrane, causing lower yields and higher purification costs. This is ultimately why the technology remains underemployed. This study aimed to develop a deeper understanding of butanol toxicity at the membrane to determine future targets for membrane engineering. Changes to the lipidome in *Clostridium saccharoperbutylacetonicum* N1–4 (HMT) throughout butanol fermentation were investigated with thin layer chromatography and mass spectrometry. By the end of fermentation, levels of phosphatidylglycerol lipids had increased significantly, suggesting an important role of these lipid species in tolerance to butanol. Using membrane models and in vitro assays to investigate characteristics such as permeability, fluidity, and swelling, it was found that altering the composition of membrane models can convey tolerance to butanol, and that modulating membrane fluidity appears to be a key factor. Data presented here will ultimately help to inform rational strain engineering efforts to produce more robust strains capable of producing higher butanol titres.

1. Introduction

Butanol is an important high-value chemical with a wide range of applications in industry. It is used as a platform chemical in the synthesis of derivatives including polymers, plasticisers, and solvents [1]. Additionally, butanol can be used as a "drop-in" substitute for petroleum, where it harbours many advantages over the more conventional biofuel ethanol, having a 30 % higher calorific value [2], increased blending capabilities, and being safer to handle. In recent years there has been an international resurgence in interest in the bioproduction and commercialisation of butanol with many international enterprises investing in related infrastructure and technologies. This primarily stems from unstable petroleum prices, concerns of energy security, and the detrimental impact of fossil fuels on the environment [3].

Several microorganisms have been used to ferment butanol with solventogenic Clostridia (mainly, *Clostridium acetobutylicum*, *C. saccharoperbutylacetonicum* and *C. beijerinckii*), native producers, being the most popular. However, widespread implementation of fermentative routes of butanol production have been hindered by the associated toxicity towards producing cells [4]. Butanol concentrations of between, 7.0–13.0 g/l result in a 50 % reduction in *Clostridium acetobutylicum* cell growth [5,6], and final concentration of butanol for non-engineered strains is generally 5.0–16.0 g/l [7]. However, these values vary greatly based on specific stains and experimental conditions. Butanol is thought to partition into the membrane and disrupt phospholipid packing leading to destabilisation, thinning and an increase in

* Corresponding author.
E-mail address: a.goddard@aston.ac.uk (A.D. Goddard).

https://doi.org/10.1016/j.bbamem.2023.184217
Received 10 May 2023; Received in revised form 17 July 2023; Accepted 17 August 2023
Available online 28 August 2023

lateral diffusion and fluidity within the membrane [8]. Guo and colleagues [9] showed butanol to interact preferentially with the phospholipid headgroup, causing thinning of the membrane and acyl chain splaying. Dysregulation of membrane fluidity can lead to leakage of intracellular components and the disruption of the maintenance of ion gradients over the cell membrane [10]. Butanol can also negatively impact membrane linked-functions and energy metabolism at concentrations below those which would cause disruptions to ion gradients [11]. Membrane integrity clearly plays a central role in butanol-mediated disruption and will likely be a focal point in the development of more tolerant strains.

Progress with engineering strains to be more tolerant and to produce more butanol has proved difficult owing to the complex stress response, and the lack of knowledge surrounding regulatory mechanisms in solventogenic Clostridia. There have been several successful examples of engineering other microorganisms such as *E. coli* and *S. cerevisiae* to be more tolerant to butanol– some of which have worked by influencing membrane composition. Butanol tolerance and membrane integrity in *S. cerevisiae* was increased following the expression of a mutated ACC1 acetyl-CoA carboxylase. This was found to be due to an increase in saturation and average lipid tail chain length [12]. Similarly, the introduction of rat elongase 2 (rELO2) (C16:0 to C18:0) to *S. cerevisiae* increased C18:1 content (but not total proportion of unsaturated fatty acids) and tolerance to several short-chain alcohols, including butanol [13]. Tan and colleagues [14] show that the expression of cis-trans isomerase (CTI) from *Pseudomonas putida* allowed for incorporation of trans unsaturated fatty acids into the membrane of *E. coli*. The incorporation of trans unsaturations resulted in increased membrane rigidity and tolerance to several alcohols, as well as unfavourable industrial conditions e.g. high temperature and acidity. These examples highlight the importance of modulating the cell membrane as a means of reducing membrane-related butanol stress. Despite these advances in non-native butanol producers, butanol yields of non-native producers are lower than required for commercial [15]. Challenges remain in engineering Clostridial membranes, not least the relatively poor characterisation of the lipidome and the historical genetic intractability. Recent developments in lipidomics approaches and genome modifications such as the 'CLEAVE™' technology developed by Green Biologics [16] open the door to rational design of strains with desirable membrane compositions. Here, we use a combination of lipidomics of native butanol producing Clostridia from industrial fermentations, coupled to in vitro and in silico approaches to determine key targets for future membrane engineering strategies. Promoting tolerance in solventogenic microorganisms will enhance the bio-production of butanol as an alternative to conventional fossil fuel routes.

2. Materials and methods

2.1. C. saccharoperbutylacetonicum N1–4 (HMT) fermentations and initial lipidomics in high and low butanol environments

Standard 48 h batch fermentations were carried out following Green Biologics internal protocols. Overnight *C. saccharoperbutylacetonicum* N1–4 (HMT) cultures were grown in reinforced clostridial media (RCM) (Oxoid), and a 10 % inoculum of this culture was used for 1.5 l fermentations. For the fermentations, cells were grown in 1.5 l TYIR (2.5 g l^{-1} yeast extract, 2.5 g l^{-1} tryptone, 0.025 g l^{-1} $FeSO_4$, 0.5 g l^{-1} $(NH_4)_2SO_4$, 10 mM MES), fermenters were set to 32 °C, 50 rpm, and a pH set point of 5.3. The fermentation was stopped after 48 h. Samples were taken every 3 h throughout for the time course experiments, with only the end point sample being taken for the high and low butanol environments. In order to induce a high or low butanol environment, cells were grown in TYIR on either 5 % mannitol for high butanol or 5 % galacturonic acid for low butanol. For the time course experiments 5 % glucose was used. For the initial lipidomics experiments, a Thermo Accucore C30 100 × 21 mm, 2.6u, (P/N 27826-102130) with a matching C30 guard cartridge C30 (10 × 2.1 mm 2.6u; P/N 27826-012105) was used to separate extracted lipids from the *C. saccharoperacetobutylicum* N1–4 (HMT) samples. Running solvent A was 60:40 acetonitrile:water (v/v), 10 mM ammonium formate and 0.1 % formic acid, and solvent B was 10:90 acetonitrile:isopropanol (v/v), 10 mM ammonium formate and 0.1 % formic acid. A gradient program over 21 min was used as follows: B 0–21 min 1 %–99 %, then isocratic for 3 min, then return to initial conditions over 0.1 min and isocreatic until 28 min. The flow rate was 350 µl min^{-1}, and the column was maintained at 40 °C. All samples were analysed in positive and negative heated electrospray (HESI) mode on a Thermo Orbitrap Fusion instrument. Full-scan MS1 data was collected in profile mode at high resolution (240,000 FWHM at *m/z* 200) over the mass range 200–1600 m/z, and data-dependent MS2 fragmentation data was collected in parallel low resolution CID and HCD modes, as centroid data. For internal mass calibration, Easy-IC was used in the positive mode whilst user-defined lock masses were used in the negative mode. The top 100 most intense peaks were retained and searched against the LipidBlast libraries. These peaks were aligned and grouped across samples, and consensus LipidBlast annotations assigned for each group, based on the best reverse dot-product scores compared to the in silico LipidBlast database. Semiquantitative comparisons are presented as peak areas, or peak areas as a percent of total area in a sample extract.

2.2. Analysis of C. saccharoperbutylacetonicum N1–4 (HMT) time course samples

2.2.1. Total lipid extraction and quantification

Total bacterial lipids were extracted using a modified Bligh and Dyer method [17]. To 50 mg pelleted cells, 500 µl of methanol at 50 °C was added. Following incubation in a sonicating water bath for 15 min, 500 µl of chloroform was added and the incubation was repeated. After the second 15 min incubation, 500 µl of 0.88 % KCl was added and the mixture was vortexed. The organic and aqueous phases were separated by centrifugation at 1000 ×*g* for 2 min. The total lipids present in the organic phase was then quantified using the Stewart Assay [18] and a standard curve of 0–50 µg of 1 POPE: 1 POPG: POPC, reading absorbance of the chloroform layer at 488 nm.

2.2.2. Thin layer chromatography

Lipid species present in *Clostridium saccharoperbutylacetonicum* N1–4 (HMT) extracts were investigated using thin layer chromatography following extraction and total lipid quantification. Along with standards, 20 µg of sample was dotted onto a silica coated aluminium TLC plates (Merck) which was allowed to dry. Following this, plates were placed into a TLC tank with a small amount of mobile phase (70 Hexane: 30 diethyl ether: 1 acetic acid; 25 chloroform: 15 methanol: 4 acetic acid: 2 H_2O) in which they were left allowing the solvent front to migrate upwards. Plates were allowed to dry before visualisation. For neutral lipids, plates were dipped into a copper sulphate solution (10 % $CuSO_4{\cdot}5H_2O$; 8 % H_3PO_4) and then baked at 150 °C for 10 min in an oven. Molybdenum blue spray reagent (Sigma-Aldrich) was used to visualise PS, PC and PG, respectively. Densitometry analysis was carried out using ImageJ.

2.2.3. Time course lipidomics

Lipid extracts were initially passed through a reversed phase Accucore™ C18 column on an UltiMate 3000 HPLC system (ThermoFisher). Running solvent A was 50 H_2O: 50 acetonitrile, 50 mM ammonium formate, 0.1 % formic acid and solvent B was 85 isopropanol: 10 acetonitrile: 5 H_2O. The gradient of solvents began with 90:10 A:B and ended with 5:95 after 21 min and was isocratic for the remaining 14 min at 90:10. The flow rate was 150 µl $min^{-1}$and the HPLC column temperature was maintained at 50 °C. For subsequent ESI-MS analysis, all samples were analysed in positive and negative ion mode on a TripleTOF® 5600 (Sciex). The ESI temperature was set to 300 °C, the mass range was 200–1600 *m/z* and the ion spray voltage of 5500 V and

−4500 V for positive and negative ion modes, respectively. An Information Dependent Acquisition (IDA) was run for MS-MS analysis – with a maximum of 5 candidate ions per cycle chosen. The instrument was calibrated using APCI Negative Calibration Solution (Sciex). Data was analysed using PeakView 2.2 (Sciex) and were additionally searched against public lipidomic libraries such as LipidMaps using Progensis QI v2.1 (Nonlinear Dynamics).

2.3. In vitro liposome assays

Liposomes were prepared using commercially purchased lipids (Avanti Polar) or extracted lipids. All preparation was carried out at temperatures above the phase transition temperatures of the component lipids. Lipids in chloroform were dried down in a round-bottom flask under a stream of nitrogen. Resulting lipid films were stored at −20 °C under nitrogen to prevent oxidisation. Lipid films were rehydrated in liposome buffer (50 mM Tris, 50 mM NaCl, pH 7.4), or in 100 mM 5(6)-Carboxyfluorescein pH 7.4 (CF) (Sigma-Aldrich) made up in liposome buffer. This was done through vortexing resulting in large multilamellar vesicles (LMV). Following this, resuspended lipid solutions were incubated for 1 h at 120 rpm shaking at a temperature of 10 °C above the phase transition temperature of the lipid components. LMVs were extruded 21 times to produce smaller unilamellar liposomes at a size of 400 or 100 nm depending on the application. For CF liposome solutions, excess unincorporated dye molecules were removed through 3 cenwash cycles: Liposomes were centrifuged at 100,000×*g* for 30 min, pellets were resuspended in liposome buffer. This was repeated twice more. For Laurdan assays, extruded liposomes were incubated with 2.5 μM Laurdan for at least 1 h at 120 rpm shaking at a temperature of 10 °C above the phase transition to allow integration into the membrane.

2.3.1. Carboxyfluorescein and Laurdan fluorescence assays

Both CF release and Laurdan assays were carried out in black 96-well plates (Greiner). CF liposomes and Laurdan liposomes were used at working concentrations of 0.25 mg/ml and 2.0 mg/ml, respectively. Plates were incubated at room temperature with occasional agitation for 10 min after which fluorescence was recorded. Fluorescence was read at the following wavelengths for CF; 485 nm and emission and 535 nm. For laurdan, the general polarisation (GP) was calculated from the ratio of emission intensities via the following equation:

$$GP = \frac{I_{485} - I_{535}}{I_{485} + I_{535}}$$

Where I_{485} and I_{535} refer to emission intensities at 490 nm and 535 nm, respectively.

2.3.2. DLS

The average liposome diameter in a solution was calculated using dynamic light scattering on a NanoBrook 90Plus Zeta in accordance with the manufacturer's instructions. Liposome samples were diluted to <0.125 mg/ml, or to an ideal counts per second of ~400 kcps.

2.4. In silico molecular dynamics

In silico techniques were used to visualise the interaction between butanol and 3 POPE: 1 POPG membrane. Initial molecular dynamic simulations utilised a coarse-grained model in which some atoms are grouped together. These were carried out in GROMACS 5.1.2 using the MARTINI 2 forcefield. The 3 POPE: 1 POPG membrane contained 336 lipid molecules and 8533 atoms in total. (90 NA, 6 CL, 4400 SOL and 5 Butanol; 126 POPE and 42 POPG molecules per leaflet). The membrane generated using insane.py underwent a short md run of 20 ns to enable relaxation and more realistic packing of the lipid beads after initial energy minimisations. Following this, 5 solvent beads were substituted for 5 butanol beads before the system's energy was minimised once again. After this, the simulation was run for 200 ns and was visualised using Visual Molecular Dynamics (VMD) [19]. The simulation was run at 293 k using a Berendsen thermostat. The Verlet cutoff-scheme was used with a Van der Waals radius of 1.1 nm. The constraint algorithm used was Lincs.

2.5. Atomic force microscopy

Liposomes extruded to 100 nm were used to make the bilayers. Approximately 100 μl of 1 mg/ml liposome solution was pipetted onto the sample freshly cleaved mica (aluminium silicate) discs, this was then incubated at room temperature for 1 h. An additional 20 μl of 10 mM Mg^{2+} was added and incubated for a further 15 min to aid final liposome rupture and form a defect free bilayer. This was subsequently washed by exchanging with approximately 100 μl dH2O (MilliQ) at least 10 times, jetting across the surface to remove excess vesicles. Samples were run using a Dimension FastScan Bio™ (Bruker) using a FastScan-D probe in liquid, tapping at a frequency of 110 kHz. The imaging buffer was fully exchanged with butanol solutions during scanning to enable the effects to be recorded instantly.

3. Results

3.1. The C. saccharoperbutylacetonicum N1–4 (HMT) lipidome alters upon butanol production

There have been, in some cases, conflicting reports of alterations in Clostridial lipidome in response to butanol. Part of this, as reported by Kolek and colleagues [20], likely stems from the differences in membrane stress from endogenous and exogenous butanol. Additionally, Clostridia are a diverse group of bacteria, even within more closely related solventogenic species [21]. It was therefore important to define the changes seen in *C. saccharoperbutylacetonicum* N1–4(HMT) upon production of butanol. To characterise these changes, fermentations producing relatively low and high concentrations of butanol were conducted. These were generated through the use of different carbon sources during fermentation with mannitol for high butanol and galacturonic acid for low butanol. When comparing the two different conditions, Fig. 1 shows a large reduction in the levels of plasmalogen-containing PE and an increase in triglycerides and the fraction of unknown lipids in positive mode. In negative mode there is an increase in amount of PG lipids and cardiolipin. It is striking that there are a large proportion of Clostridial lipids not present within current databases, making assignment difficult. Whilst *C. saccharoperbutylacetonicum* has not been reported to produce ceramides, we identified a small proportion of these lipids via mass spectrometry assignments. Further work will be required to determine if these are from the media, represent misassignment of unknown Clostridia lipids or represent novel biology.

3.2. Temporal changes in the lipidome correlate with butanol production

The above data represents "end point" lipidomes under high and low butanol conditions. However, industrial fermentations involve a combination of cell growth and solvent production which are not constant. Therefore, the lipidome of *C. saccharoperbutylacetonicum* during an industrial fermentation conducted by Green Biologics Ltd. was characterised. The time points selected are shown in Fig. 2, along with associated fermentation data. The black arrows along the OD_{600} denote the timepoints, each of which corresponds to different part of the cells' growth cycle: 5 h, end of lag and start of log; 10 h, mid log; 15 h, midpoint of fermentation; 23 h beginning of stationary phase growth; 35 h, start of death phase. There is a steady increase in butanol concentration throughout the fermentation (indicating that the cells have not sporulated) which will likely impact the lipids present. It should be noted that there is no distinct acidogenic or solventogenic phase (solvent synthesis occurs concurrently with acid synthesis) in this particular

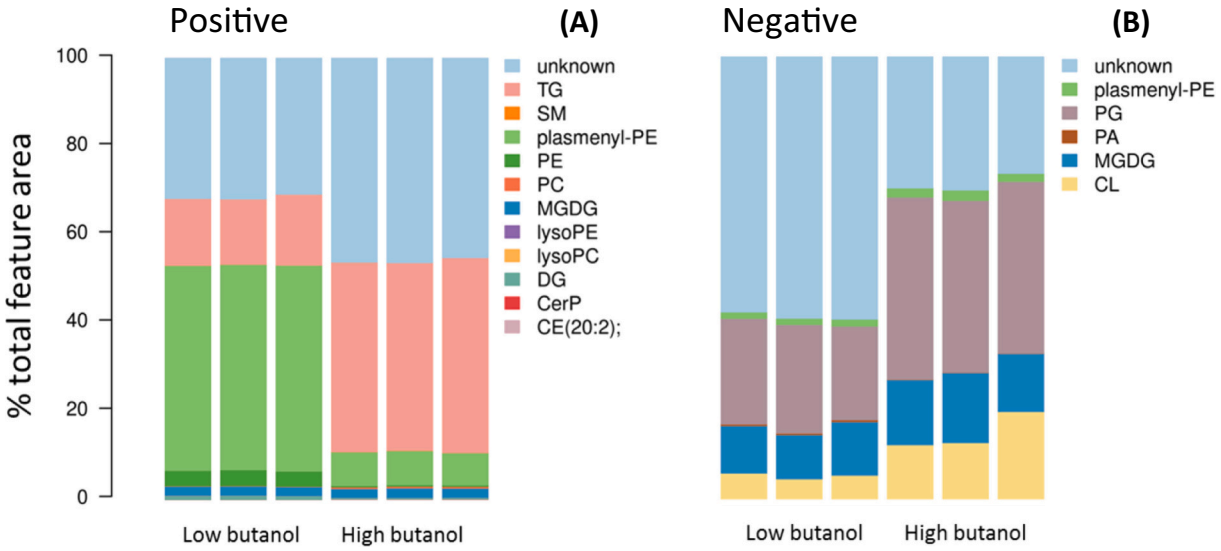

Fig. 1. Lipid class coverage for several *C. saccharoperbutylacetonicum* grown in environments with different butanol concentrations. Three technical repeats are shown for both high and low butanol. A C30 column was used for both positive mode (A), and negative mode (B). The lipid classes are as follows: TG, triacylglycerides; SM, sphingomyelins; PS, phosphatidylserines; PE, phosphatidylethanolamine; PG, phosphatidylglycerol; PC, phosphatidylcholine; PA, phosphatidic acid; MGDG, Monogalactosyldiacylglycerol; DG, diacylglycerides; CL, cardiolipin; CerP, ceramides; CE, sterol. 'Plasmenyl-'denotes the presence of plasmalogen containing acyl. Lyso lipids contain only one acyl chain. Light blue represents unknown lipids species.

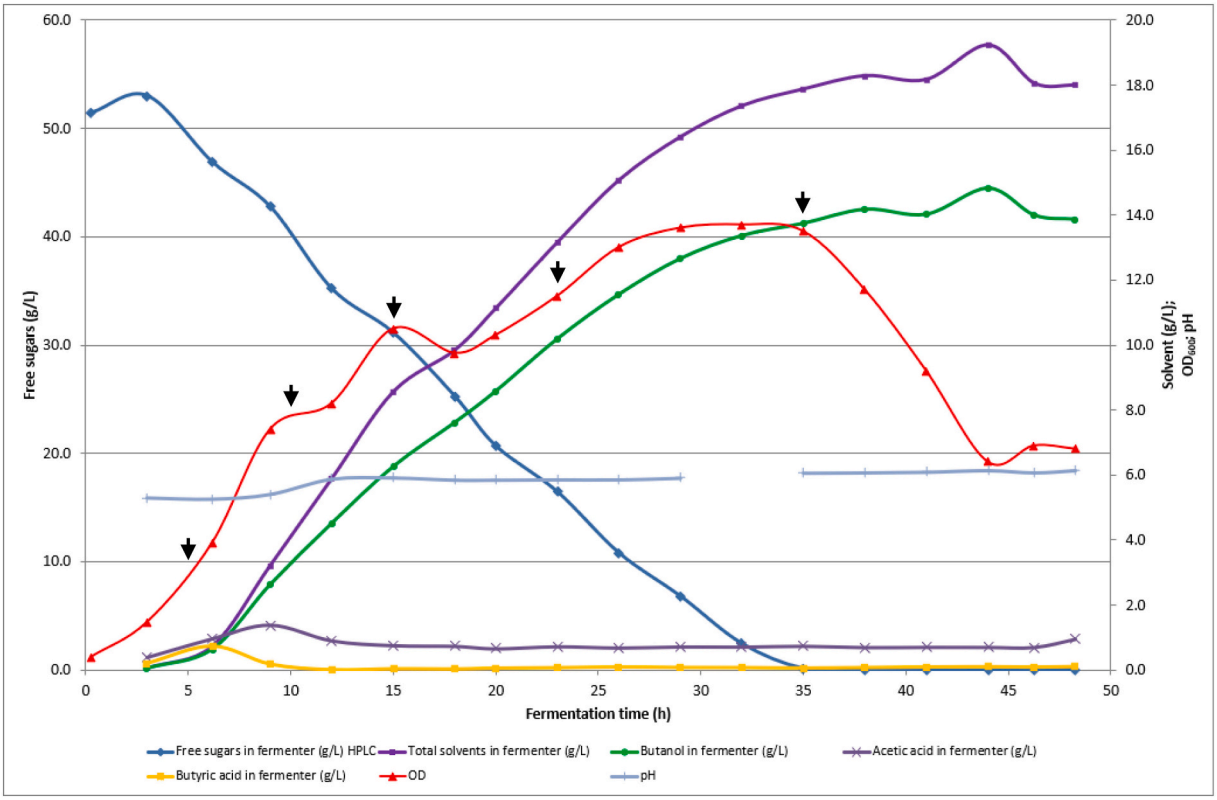

Fig. 2. *Clostridium saccharoperbutylacetonicum* N1–4 (HMT) fermentation characterisation. The black arrows denote the timepoints where biomass was harvested for lipidomic analysis. They were chosen to reflect different points in the life cycle of the cells. Timepoints: 0 h, seed; 5 h, end of lag and start of log; 10 h, mid log; 15 h, midpoint of fermentation; 23 h beginning of stationary phase growth; 35 h, before death phase. pH was not recorded for the 32 h timepoint.

strain.

Thin layer chromatography (TLC) was used to initially characterise the head groups of lipids throughout the fermentation. A standard containing 20 μg (an equal mass to the sample loaded) of POPE, POPG or POPS was run. In each case, the mobile phase was 25 chloroform: 15 methanol: 4 acetic acid: 2 H_2O/POPE was visualised using ninhydrin and POPG and POPS with molybdenum blue. Spots were quantified relative to the zero-hour timepoint using ImageJ [22]. No POPC was detected (data not shown) which is in line with previous works which did not detect phosphatidylcholine lipids in a range of Clostridia [23].

Both POPS and POPG were detected in all samples and the levels of POPG appear to increase steadily through the course of the fermentation (Fig. 3). This increase approximately correlates with the increase in butanol concentrations seen in Fig. 2. The levels of POPG were highest in the later portion of the fermentation and were significantly higher at 15 h and 35 h than compared to the start of the fermentation. Levels of POPS appear to somewhat reflect growth in the cells (Fig. 3), i.e. POPS is at its highest when there would be the highest amount of proliferation in the culture. Despite this trend, there was found to be no significant difference at any of the timepoints.

The same samples were also investigated with HPLC-ESI tandem mass spectrometry to investigate broad changes of all lipids classes across fermentation (Fig. 4). Due to the large scope of these experiments, standards were not used and thus, the interpretation of this data is limited and should be seen as auxiliary to the TLC and earlier lipidomic experiments. Furthermore, the lack of standards means that determining quantifications is difficult, and thus data is expressed as a relative abundance of annotated features. Samples were run in both positive and negative ionisation mode, and the data was analysed using Progenesis QI 2.1 (Nonlinear Dynamics) with features annotated using the LipidMaps database. Based on negative ionisation the lipidome of these *C. saccharoperbutylacetonicum* N1–4 (HMT) samples appears to contain mainly ethanolamine species (phosphatidylethanolamine (GPEtn, PE, (PE(O-)) and plasmanylethanolamine (PE(P-)), phosphatidylglycerol (GPGro)), phosphatidic acid (GPA) and Monogalactosyldiacylglycerol (MGDG)) (Fig. 4A). The positive ionisation mode also shows large relative amounts of PE, sugar-containing species (monogalactosyldiacylglycerol and digalactosyldiacylglycerol), and diacylglycerol and triacylglycerol. Additionally, a small amount of phosphatidylserine (GPSer) and GPA was detected (Fig. 4). This is broadly in line with the lipidomes observed in Fig. 1.

Whilst the data shows no significant differences between timepoints, it provides a useful quantitative narrative of changes during the fermentation. Relative abundances in the positive ionisation mode appear to remain similar across all time points with perhaps being a small increase in the sugar containing lipids and a small decrease in DG levels. In negative ionisation mode levels of GPA, GPGro, and MGDG appear to increase at the later time points in fermentation, whereas ethanolamine containing species appear to decrease across fermentation. This increase in phosphatidylglycerol was seen in the previous lipidomics and later TLC experiments and a reduction in PE species was also seen in the previous lipidomics experiments. Overall, this suggests that the balance of PE and PG-containing lipids could provide an engineering target to increase butanol tolerance.

3.3. Butanol integrates into lipid membranes and interacts with phospholipid head groups

Due to the number of unidentified lipids in *C. saccharoperbutylacetonicum* and the inherent challenges of membrane engineering, especially when the biosynthetic pathways may not be fully characterised, it is important to understand the biophysical properties of the membrane to open new avenues to membrane modulation to produce desirable characteristics. Liposomes represent a well-established system for studying the effect of membrane-active compounds [24]. They allow precise control over lipid composition and measurements of both integrity and fluidity using fluorescent assays.

To characterise the effect of butanol on liposome membranes, dynamic light scattering (DLS) was employed. Liposomes composed of POPC or 3 POPE: 1 POPG (as a Clostridial membrane model) swelled upon butanol exposure in a concentration dependent manner (Fig. 5), which reaffirms the notion that butanol causes damage by perturbing interlipid interactions. As butanol is more viscous than water, increasing the proportion of butanol in these DLS experiments may have resulted in a perceived increase in swelling due to an increase in solution viscosity. A control consisting of 100 nm inert polystyrene standards were used to investigate this. The polystyrene standards are not subject to direct butanol-mediated swelling but will be impacted by the viscosity of the solution. It was found that up to 50 mg/ml butanol had no significant impact on the measured sizes of these polystyrene standards. These data suggest that either butanol intercalates into the membrane, as suggested previously [9] or decorates the surface of the liposomes, increasing their hydrodynamic radius. To differentiate between these possibilities, in silico modelling was carried out. Coarse-grained modelling using the MARTINI 2 force field was employed to simulate and predict the spatial location of butanol-phospholipid interaction (Fig. 6). The simulation was run for 200 ns to enable sufficient time for and interaction to be realised. In coarse-grain models, atoms are grouped together to form beads. This practice reduces the computing power required and enables longer simulations. Fig. 6 shows the progression of the simulation from a starting point at 0 ns to the end of the simulation at 200 ns. Butanol was represented as a single bead (enlarged red bead) and can be seen in the starting panel (0 ns) to be occupying several locations ranging in distance from the phospholipids on both sides of the bilayer. Butanol molecules were diffusing freely around the bulk solvent, however once in close proximity to the membrane they moved into the headspace region and existed around the phosphate group of the phospholipids (orange beads). There appeared to be a range of butanol localisations once an interaction had been established, from the upper acyl chains to the head group regions of the phospholipids (green beads represent POPG and blue beads represent POPE. The headgroup region pertains to the green and blue bead on the outer side of the phosphate groups, closer

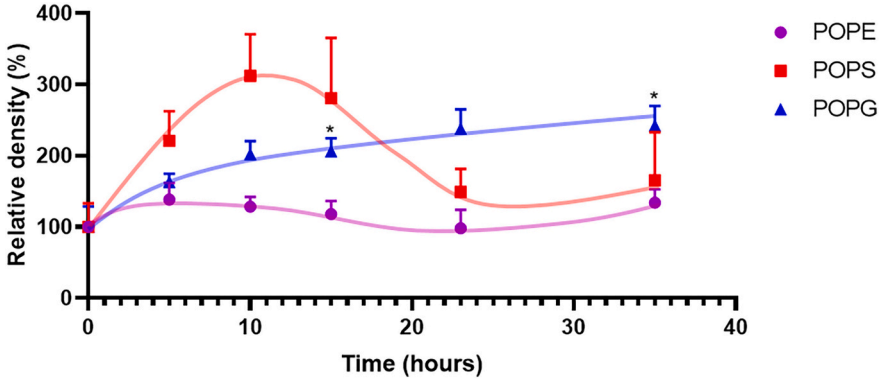

Fig. 3. Thin layer chromatography of *Clostridium saccharoperbutylacetonicum* N 1–4 (HMT) total lipid extracts from time points throughout fermentation. Lipids analysed were POPE (purple, circle); POPG (blue, triangle); POPS (red, square). Total bacterial lipids were extracted using a modified Bligh and Dyer method and quantified using the Stewart Assay. Equal concentration of lipids were run. A mobile phase of 25 chloroform: 15 methanol: 4 acetic acid: 2 H_2O was used. POPE was developed using ninhydrin reagent (B) POPG and POPS developed using molybdenum blue. The concentrations were determined by densitometry analysis was using ImageJ, and normalised to 0 h timepoint. 3 technical repeats of 2 biological repeats were carried out. Error bars represent SEM for 2 biological repeats, with only the positive error being shown. * = $p < 0.05$ compared to 0 h, using an unpaired *t*-test assuming equal SD between samples. Lines for each data set are not fitted to data points and are merely guides. They have been included to increase the ease of interpretation.

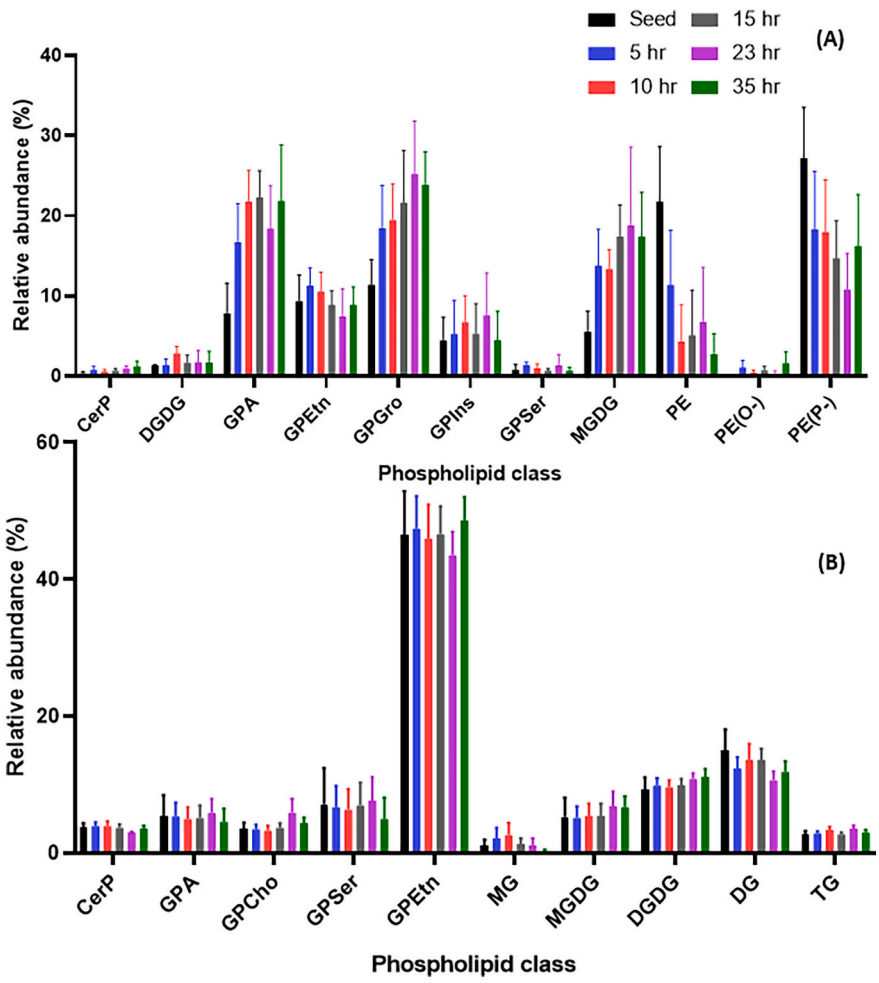

Fig. 4. Abundance of lipid classes throughout *Clostridium saccharoperbutylacetonicum* N 1–4 (HMT) fermentation. (A) negative ionisation mode (B) positive ionisation mode. The lipid classes are as follows: TG, triacylglycerides; SM, sphingomyelins; PS, phosphatidylserines; PE, phosphatidylethanolamine; PG, phosphatidylglycerol; PC, phosphatidylcholine; PA, phosphatidic acid; MGDG, Monogalactosyldiacylglycerol; DG, diacylglycerides; CL, cardiolipin; CerP, ceramides; CE, sterol. '(P-)' denotes the presence of plasmalogen containing acyl. The proportions of each lipid class was calculated as a percentage of total abundance of annotated species in the LipidMaps database using Progenesis QI v2.1. (Nonlinear Dynamics). 3 technical repeats of 2 biological repeats were carried out. Error bars represent SEM for 2 biological repeats, with only the positive error being shown.

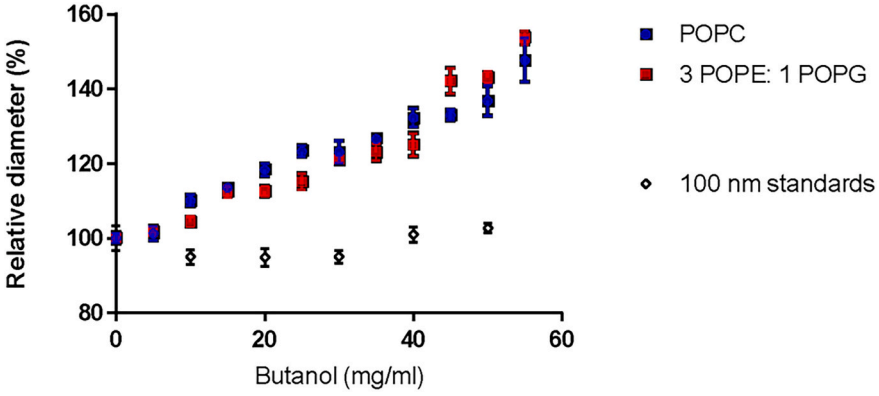

Fig. 5. The normalised diameter of liposome models POPC and 3 POPE: 1 POPG, and 100 nm polystyrene standards in response to butanol. Butanol exposure causes liposomes to swell. The variation seen in the response to butanol is within the manifesting error of ±3 %. Liposome size was read using dynamic light scattering following butanol exposure. Samples were diluted to an ideal counter per second as determined by the software used. Diameters were normalised to 0 mg/ml. $N = 3$, ±1SEM.

to the bulk solvent). At 1 ns there are 3 butanol beads occupying this area and as the simulation progresses to 10 ns and 20 ns it can be seen that and additional 2 butanol beads enter into this zone too (one at 10 ns and one at 20 ns). Integration of butanol into the membrane is clear and leads to the possibility of (transient) pore formation which would lead to cell leakage and death.

3.4. Butanol exposure increases both membrane fluidity and reduces membrane integrity in a lipid-dependent manner

The use of liposomes as model membranes enables the production of bespoke membrane compositions and allows the for the inclusion of key membrane lipids identified from the lipidomics data. Notable observations were an increase in chain length and an alteration in PE:PG ratio. Additionally, plasmalogens and membrane fluidity appear to be important membrane characteristics involved in butanol tolerance [25–28]. The consequences of butanol exposure were measured using a combination of CF release (as a measure of membrane integrity) and laurdan GP (as a proxy for membrane fluidity). Membrane integrity is measured by leakage of concentrated/quenched CF dye from inside a liposome, which becomes diluted in the surrounding buffer as it leaks out through the weakened membrane and dequenches/fluoresces.

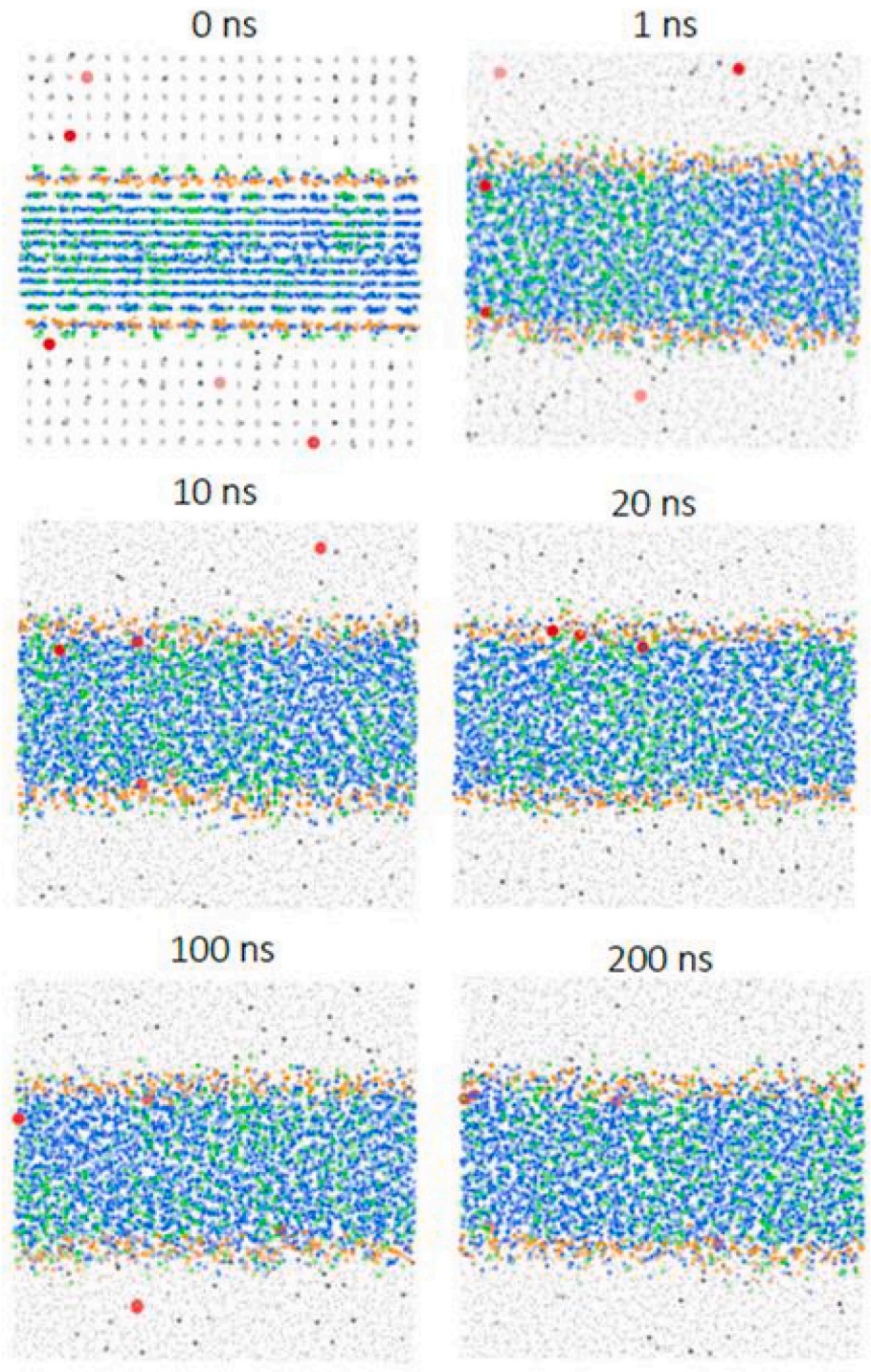

Fig. 6. Coarse-grained molecular dynamic simulation of butanol interacting with a 3 POPE: 1 POPG membrane. The coloured beads represent groups of atoms (colour, atom group;): red, butanol; water, light grey; ions, Dark grey; POPE, Blue; POPG, Lime green; PO42-group, Orange. The 0 ns panel shows the starting positions. By 20 ns all butanol molecules were within the headgroup region, however later in the simulation butanol molecules were found within the bulk solvent, suggesting a non-permanent interaction with the membrane. Simulations were carried out in GROMACS 5.1.2 with the MARTINI 2 forcefield. The system was run for 200 ns and visualised using Visual Molecular Dynamics (VMD) (University of Illinois).

Membrane fluidity was measured by changes in Laurdan GP values. The GP values are proportional to the shift in intensities of emission spectra, caused by a change in the local environment of the laurdan probe (greater exposure to water due to increased membrane fluidity). GP values range between 1 and −1, and lower values indicate higher membrane fluidity. Both membrane permeability and membrane fluidity were seen to increase (increasing CF fluorescence and decreasing GP value, respectively) with increasing butanol concentrations in all lipid compositions tested.

Initially, the effect of headgroup species on butanol tolerance was investigated using liposome membrane models of varying headgroup composition (Fig. 7). Both PE and PG headgroups constitute major components of the lipid membrane in Clostridia [23], and thus 3 POPE: 1 POPG is considered to be a simplified model membrane composition [29]. Liposomes made from 3 POPE: 1 POPG released significantly less ($p < 0.05$) CF than POPC liposomes within a biologically relevant range of butanol concentrations (15–30 mg/ml) (Fig. 7A). Interestingly, above 30 mg/ml there was found to be no significant difference between the two headgroup compositions in terms of CF release. These data demonstrate that alterations in the lipid composition affect butanol disruption of membranes within a biologically relevant range.

The ratio of POPE to POPG was highlighted within the lipidomics data as important and was investigated by spiking in more POPG to the 3 POPE: 1 POPG model during liposome preparation (Fig. 7C and D). In

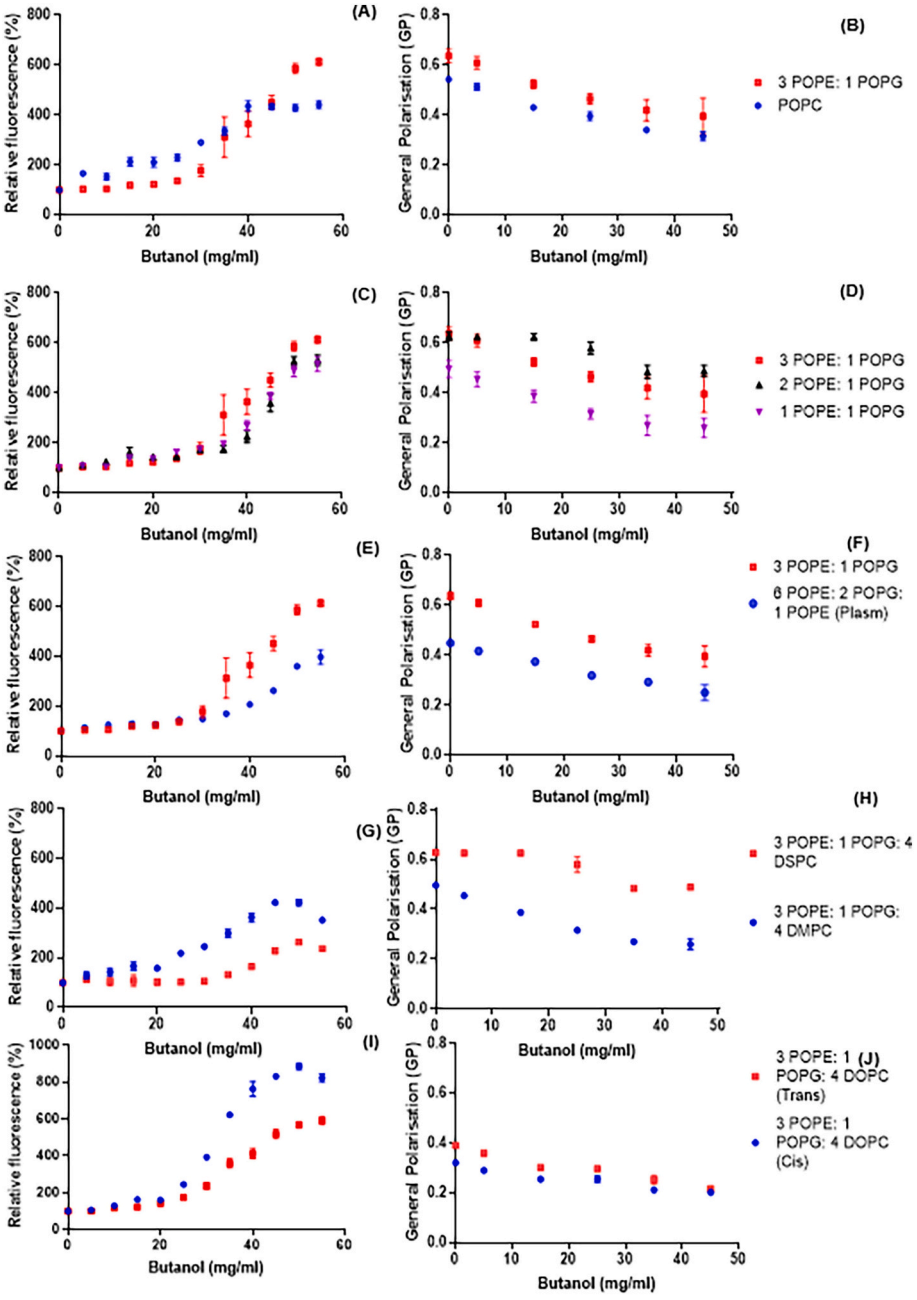

Fig. 7. Carboxyfluorescein (CF) fluorescence dye release and laurdan probe general polarisation (GP) of membrane models with different lipid compositions following butanol exposure. CF fluorescent dye was loaded inside liposomes with different lipid compositions. These were then exposed to a range of butanol concentrations and the fluorescence was recorded. 3 POPE: 1 POPG was used as a base composition. Prior to liposome generation, other lipid species were added to 3 POPE: 1 POPG in an equal amount (mg/mg), generating a range of compositions. CF release assay comparing **(A)** POPC and 3 POPE: 1 POPG **(C)** POPE: POPG ratios **(E)** 3 POPE: 1 POPG to 6 POPE: 2 POPG: 1 PE(Plasmalogen) **(G)** 3 POPE: 1 POPG: 4 DMPC and 3 POPE: 1 POPG: 4 DSPC **(I)** 3 POPE: 1 POPG: 4 DOPC (Δ9-Cis) and 3 POPE: 1 POPG: 4 DOPC (Δ9-Trans). Fluorescence was measured on a Mithras LB940 with the following wavelengths for CF; Excitation: 485 nm Emission: 535 nm. N = 3, ±1SEM. GP values comparing **(B)** POPC and 3 POPE: 1 POPG **(D)** POPE: POPG ratios **(F)** 3 POPE: 1 POPG to 6 POPE: 2 POPG: 1 PE(Plasmalogen). **(H)** 3 POPE: 1 POPG: 4 DMPC and 3 POPE: 1 POPG: 4 DSPC **(J)** 3 POPE: 1 POPG: 4 DOPC (Δ9-Cis) and 3 POPE: 1 POPG: 4 DOPC (Δ9-Trans). Fluorescence was measured on a Mithras LB940. The laurdan fluorescent probe was added to aqueous liposome solutions after lipid film rehydration. After a 1 h incubation period, the liposomes were exposed to a range of butanol concentration and the fluorescence was recorded. The GP value was then calculated using the equation described in Section 2.3.1 Carboxyfluorescein and Laurdan fluorescence assays and laurdan fluorescence assays. Statistical analysis carried out using an unpaired *t*-test assuming equal SD between samples.

the biologically relevant range of <30 mg/ml butanol, there appears to be little difference in CF fluorescence following the inclusion of more PG in the forms of 1 POPE: 1 POPG and 1 POPE: 3 POPG. Above this range however, both models with additional PG appear to have slightly lower fluorescence than 3 POPE: 1 POPG. Whilst there was no significant difference from 3 POPE: 1 POPG liposomes for any data, it supports the hypothesis that the PE:PG ratio is potentially important for protection from butanol stress. Interestingly the was no correlation seen with the different ratios of POPG and the fluidity measured by the laurdan values. 2 POPE: 1POPG appears the most rigid, then 3 POPE: 1 POPG, with 1 POPE: 1 POPG being the most fluid, having the lowest GP values.

Plasmalogen lipids contain a vinyl-ether bond at the sn-1 position [30] and may be involved in mitigating butanol damage. This is based on their ability to pack closer together and form more ordered and more rigid structures than diacyl lipids [31]. The substitution of 12.5 % (mass) POPE for POPE which contained a plasmalogen also appeared to reduce CF leakage. Liposomes containing the plasmalogen species had significantly lower fluorescence at high butanol concentrations (>45 mg/ml) (Fig. 7E). However, there appeared to be no significant difference in CF leakage in the biologically relevant ranges of butanol (15–30 mg/ml). Additionally, the fluidity of plasmalogen containing species was significantly higher than 3 POPE: 1 POPG at all butanol concentrations (Fig. 7F). This combining with the CF leakage data suggests that overall membrane fluidity alone is not the sole determining factor of membrane integrity.

Membrane fluidity has emerged as a key theme in butanol tolerance. Alterations to the fatty acid region of the phospholipids were designed to influence fluidity as a means of investigating the impacts of fluidity on butanol toxicity. For these experiments, 3 POPE: 1 POPG was used as a base composition, into which 50 % (w/w) of another lipid species was spiked. Firstly, the length of the acyl chains was investigated whereby either DMPC (14 carbons) or DSPC (18 carbons) (Fig. 7G and H). Secondly, the degree of saturation and geometrical isomerism of any unsaturated bonds was investigated using variants of DOPC (Δ9-Trans or

Δ9-Cis) (Fig. 7I and J). CF leakage was found to be significantly higher ($p < 0.001$) in 3 POPE: 1 POPG: 4 DMPC than in 3 POPE: 1 POPG: 4 DSPC liposomes following butanol exposure >25 mg/ml. Similarly, liposomes with the cis geometric isomer were found to release significantly more ($p < 0.02$) CF in response to butanol (>30 mg/ml) than the trans isomer. Additionally, the was a large difference seen in the fluidity (Fig. 7H) of the two respective membrane compositions, with those containing DSPC being significantly less fluid in comparison to those containing DMPC.

Taken together, these data suggest that generally alterations to increase membrane rigidity are protective against butanol permeabilization. Although this was not seen with every composition tested – it may provide a starting point for membrane engineering. Additionally, CF assays show that perturbation to the membrane which leads to leakage, a process that likely occurs with the cellular components in Clostridia. However, these data do not directly confirm butanol generates membrane pores.

3.5. Atomic force microscopy directly demonstrates butanol-induced pore formation

Atomic force microscopy was employed to investigate changes to the physical structure and mechanical properties of the membrane following butanol exposure. A fluid POPC monolayer was formed successfully on mica which appears as a smooth featureless surface (data not shown), but a force curve (Fig. 8b) reveals the characteristic signature of a fluid phase bilayer. Briefly, this has a point of first contact about 6 nm above the mica surface (marked with arrow), compression of the bilayer which rapidly stiffens with the applied force rising to about 4 nN, compressing the bilayer to about half thickness (2.5 nm). At this point there is a breakthrough event when the applied force overcomes the hydrophobic forces holding the bilayer together, and the probe moves suddenly to the mica surface. The retract curve (red) reveals bilayer fluidity due to reformation of the bilayer as the downwards force reduces, expelling the

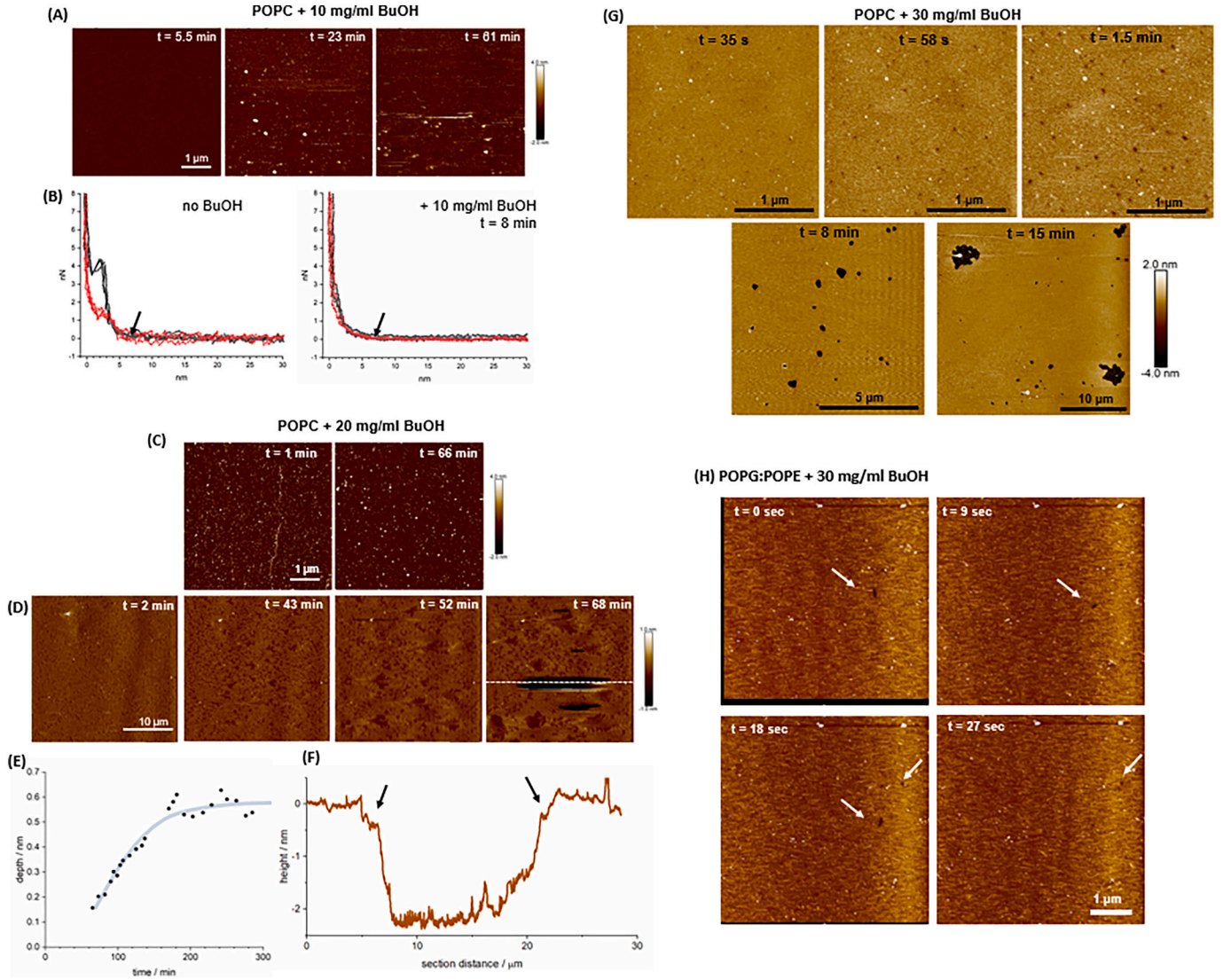

Fig. 8. (8A) 5 µm AFM scans of a POPC bilayer with added 10 mg/ml butanol. An initially featureless membrane roughens and eventually blebs after 15 min. (8B) AFM force spectroscopy curve before and after addition of 10 mg/ml butanol showing drastic reduction in structural integrity of bilayer, although it is still intact. Points of first contact are indicated by arrows. (8C) 5 µm AFM scans of a POPC bilayer with added 20 mg/ml butanol. Here blebs form immediately, but are thereafter quite stable, indicating immediate partitioning of butanol into the membrane. (8D) 30 µm scans, but with a much enhanced contrast of the bilayer surface reveals patches of further weakness and disturbance, causing the AFM probe to occasionally penetrate. (8E) the patches grow in size and depth to a maximum of 0.6 nm. (8F) a line section from the scan line indicated by the white dashed line in (8D) at 68 min, showing bilayer depth is 2.4 nm. Arrows indicate the edges of the surface depressions either size of the bilayer tear. (8G) are AFM scans at 30 mg/ml butanol showing membrane poration. They start at a reasonable high resolution to image the initial small pores forming, before zooming out to track the ever increasing growth of the full depth pores. (8H) POPG:POPE membrane challenged with 30 mg/ml butanol. Sequential frames shown from a high speed AFM movie where only very small and transient pores could be detected moving rapidly and then closing up.

probe from the bilayer and pushing it back to the surface. This effect is only observed in highly fluid bilayers. Upon addition of 10 mg/ml butanol the surface has slightly roughened with some small mobile features by 5 min, and then accompanied by minor blebbing of nanoscale vesicles after 15–20 min (Fig. 8A) driven by expansion of the membrane as butanol molecules insert into the bilayer. A surface supported bilayer cannot easily expand or contract its surface area due to friction across a large area, so a small increase in area due to inserting molecules has to be relieved by blebbing, which in a free vesicle or cell would result in a slight expansion that could be accommodated. The force curve shows a vast decrease in structural integrity after 10 mg/ml butanol addition. First contact (arrowed) is at approximately the same point 6 nm above the mica surface, the bilayer has not collapsed, but it compresses more easily for a given force, it is weaker. The resistance and breakthrough event is almost entirely abolished bar a small final breakthrough to the surface at 3 nN. It should be noted that these force spectroscopy curves are quite noisy, and were acquired during the high speed AFM experiments on a set-up not optimal for force curves. Additionally, there is less force applied from the reformation of the membrane as the probe retreats, reflecting the force response upon approach.

Exposure to 20 mg/ml butanol caused rapid surface blebbing in the first 5 μm scan (Fig. 8C), and the occasional tubule. The surface vesicle structure is dynamic, gradually developing over the course of an hour, but not much changes to the number of blebs. Zooming out to a 30 μm, but at the same time increasing contrast in the plane of the bilayer surface, reveals further detail in the bilayer (the blebs almost disappear at this lateral scale). Shallow depressions form immediately, but then grow in size up to 5 μm across and 0.6 nm deep (Fig. 8D). Although the depression form immediately, they are too small and shallow to obtain a reliable depth, and it is only after about an hour this is possible. After this point they became deeper, from 0.15 nm to 0.6 nm (Fig. 8E). The depressions are physically weaker still than the surrounding membrane, causing the AFM probe to occasionally fall through to the surface and tear the membrane. This revealed a bilayer thickness of 2.2 nm (Fig. 8F). The edges of the depression to either size of the bilayer tear are arrowed (Fig. 8F). This could be an indication of interdigitation, or reflecting the much weakened bilayer that immediately compresses to the ≈2.5 nm thickness with minimal force. Despite the further weakness in structure, the bilayer remains intact.

At 30 mg/ml butanol small depressions begin to form immediately, 30–50 nm diameter and 0.5 nm deep at 35 s, deepening to 1.5–2 nm at 1.5 min. Over time, and progressively zooming out to follow the process, the bilayer becomes fully porated, the pores growing to 5 μm after 15 min. A higher concentration of 6 % butanol resulted in a very rapid dissolution with rapidly moving circular dissolution fronts and detachment of the bilayer from the support, complete in about 30 s (data not shown). This is similar to a detergent-type mechanism.

Finally, a bilayer consisting of POPG:POPE was deposited on the mica, and imaged in the same concentrations of butanol as above. 10 mg/ml and 20 mg/ml butanol had no observable effect, resulting in perfectly smooth bilayers (data not shown). At 30 mg/ml butanol the bilayer roughened slightly with a few surface blebs forming, similar to the very early stages of 10 mg/ml butanol on POPC. Small pores of 10–30 nm diameter could be detected in the fast scanning AFM (Fig. 8H, arrowed), but these were very transient, only existing for up to a minute and moving around rapidly before closing up again. At 6 % butanol the POPG:POPE bilayer experienced a similar detergent like removal.

4. Discussion

Butanol represents an effective biofuel alternative to petroleum, however the process of its bioproduction is hindered by low yields due to product toxicity. Enhancing the tolerance of solventogenic Clostridia to butanol is paramount if this method is to be competitive with conventional means of obtaining butanol using petroleum-derived products. This study demonstrates lipidomic changes occur in *C. saccharoperbutylacetonicum* in response to butanol during fermentation and, using in vitro and in silico approaches, generates a model for how these changes are protective on a molecular level. A similar phenomenon has also been seen in *S. cerevisiae* growth during ethanol fermentation, suggesting head group composition, as well as membrane thickness, plays a fundamental role in microbial solvent adaptation [32]. Butanol has been shown to present a holistic toxic effect on membranes altering the permeability, fluidity and diameter of model membranes. This is compounded by changes seen with AFM, where membranes become softer and lose mechanical strength. Similar effects on SOPC membrane properties have been seen with butanol using micropipette aspiration, where butanol exposure reduces interfacial tension and reduce membrane thickness and mechanical moduli [33].

Butanol appears to integrate into the cell membrane, causing an increase in fluidity, presumably by disrupting lipid-lipid interactions and, at higher concentrations, leads to pore formation and eventual cell death. From our molecular dynamics simulations, it appears that, at least for a proportion of the butanol molecules (e.g. between 20 ns and 100 ns), the integration may be transient, suggesting a dynamic equilibrium between butanol in the aqueous and lipid phases. This would be logical given the short chain length of butanol. Butanol was found to cause an increase in relative diameter of liposome models in a concentration dependent manner but cannot fully solubilise membrane at concentration below phase-separation with water (<60 mg/ml). This idea that butanol molecules intercalate into the membrane and disrupt the interlipid interactions, resulting in swelling, is also supported by in silico experiments. Butanol's amphipathic structure matches that of a phospholipid enabling it to interact with both the apolar acyl chain and the polar phospholipid head group concurrently [27,34]. A case can be made for butanol having a detergent-like mechanism of membrane perturbance. Like butanol, detergents possess an amphipathic structure and also cause an increase in the size of vesicles without solubilising them [35]. Butanol has previously been used as a membrane protein extractant for its detergent-like action resulting in solubilisation of membrane proteins. Due to its lipophilicity and limited water solubility, butanol is able to extract membrane proteins into aqueous buffers with low levels of denaturation [36]. Based on this, it is possible that any butanol mediated membrane protein damage stems from a perturbance to local membrane stability and inter lipid interactions. Further studies are required into the effects of butanol on membrane proteins, but any solubilisation is likely accompanied by significant disruption of bilayer integrity. Additionally, whilst we cannot completely rule out any osmotic effects of butanol on bilayer stability, we believe its hydrophobic nature, and low contribution to overall osmolarity at the concentrations produced in fermentation, strongly point to intercalation into the membrane being the major driver of toxicity.

Any membrane engineering approach will need to be protective against either the integration of butanol into the membrane or the effects on membrane fluidity. The characteristics and packing of phospholipid head groups is likely important in controlling the initial partitioning of butanol into membranes and here, we propose that the PE:PG ratio is important in butanol tolerance. The reduced disruption seen in POPE: POPG bilayers compared to POPC may be due to an increase in resistance against butanol intercalation. This would act to mitigate the disruption of acyl chain association and help to maintain fluidity. Molecular dynamic simulations comparing POPE: POPG bilayers in a 3:1 M ratio with POPC bilayers indicate some different physical properties between the bilayers which could account for the increased resistance seen in POPE: POPG [29]. Firstly, the packing of the acyl chains in the upper regions of POPE: POPG is greater compared with POPC. This is indicated by both POPE and POPG lipids having more neighbouring lipids than POPC. It should be noted that the number of neighbouring atoms become comparable between the lipid species beyond carbon 10 in palmitoleic acid and carbon 5 in oleic acid. Hence, this increase in density of POPE: POPG only applies to the upper regions of the acyl chains. However, this may limit the intercalation of butanol

into the membrane if lipids are more closely packed together at point of insertion. Secondly, POPE and POPG form more intermolecular water bridges than PC lipids. Water bridges are where a water molecule is concurrently hydrogen bonded to two lipids and may also add to membrane [37,38]. Additionally, there was found to be 34 % more hydrogen bonds formed by PE in a POPE: POPG mixed system than in a pure PE system, resulting in greater stability at the interfacial region [39]. POPE and POPG lipids are closer together; due to the larger distance between PC-PC lipids, intramolecular water bridges become more likely than intermolecular water bridges [29]. Cheng and others [40] found that POPE: POPG bilayers in a 1:1 ratio were more resistant to insertion of several variants of the antimicrobial peptide, aurein than PC/PG bilayers. It was concluded that this was due to the more complementary orientations of POPE and POPG phospholipids in POPE: POPG bilayers. These data reaffirm the importance of altered head groups for butanol sensitivity, despite being a comparatively unexplored area [10]. It is possible that electrostatic interactions also play a role in tolerance to butanol. However, given the complex nature of the membrane and the fact that there are still a relatively large proportion of unidentified lipids in some of the lipidomic analyses, it is difficult to propose a precise model here. What seems clear is that alter head group composition (and consequential interactions) are key to modulating butanol tolerance.

An increase in the portion of PG relative to PE in the membranes may result in reduced membrane permeability and higher solvent tolerance through increasing the average headgroup area [29]. Based on this, it is likely that the increase in relative PG% across fermentation time points is an adaptive response to increasing butanol concentrations. From the data in this study, phosphatidylglycerol lipids may be involved in the butanol response. Hence, engineering pathways related to PG lipid synthesis could be an attractive route for producing a more robust strain. Similar adaptations to solvent stress have been recorded previously, with PG levels in *E. coli* increasing in response to ethanol [41]. In the presence of toluene, levels of cardiolipin (CL) (PG is a precursor to for CL synthesis) were found to be higher in *P. putida*. Additionally, there was also a transition of unsaturated bond isomerism from cis to trans [42]. Greater portions of PG and CL in bacterial membranes may represent a possible route for developing more tolerant butanol producers. Previously, cardiolipin (CL) has been reported to be a major component of the *C. saccharoperbutylacetonicum* membranes [23]. Lipidomic analysis shows levels of CL were higher in the high butanol environment than in the low butanol environment suggesting a potential involvement of this lipid too. This is likely based on the similarities between the structures of PG and CL (CL is formed by the condensation of two PG molecules and contains four acyl chains with one glycerol headgroup). PG and CL are both negatively charged lipids and likely have a similar effect on membrane properties because of this. Therefore, it could be assumed that they act in a similar way and a both protective against butanol. Recent transcriptomics analysis of *Clostridium beijerinckii* shocked with butanol show alterations to the expression of lipid synthesis genes [28]. Genes related to the synthesis of CL and lyso-PG had higher expression following butanol shock, whereas genes related to LPA, PA, PS and PC had lower levels of expression. This increase in CL and PG species biosynthesis enzymes supports the above changes seen in the TLC and lipidomics analysis.

Whilst membrane lipid composition engineering remains in its infancy, there are examples of success in bacteria. Tan and colleagues [43] overexpressed phosphatidylserine synthase (PssA) *in E. coli*. The resulting strain was more tolerant to several industrially relevant compounds including acetate, ethanol and octanoic acid. There was also a concurrent increase in chain length which may amplify tolerance, likely through mediating fluidity and reducing solvent insertion into the membrane. Despite a limited beneficial effect following butanol exposure, this study highlights the benefits associated with engineering head group biosynthesis pathways, revealing it to be a viable strategy.

Butanol integrates into the membrane; it is therefore important to protect against its fluidising effects. Membranes with a greater proportion of saturated fatty acids will be more ordered and rigid, with individual lipid molecules packing together better (as the presence of unsaturation results in kinked acyl chains). This enables stronger intermolecular Van der Waals forces, reducing fluidity and countering the effects of butanol. Similarly, increasing the length of the acyl chains will result in more inter lipid forces and allows for stronger interactions with acyl chains in the adjacent leaflet. Bilayers containing shorter chains are freer to move due to reduced interactions between acyl chain ends of opposite leaflets [44]. The bond angle of an unsaturated bond in the trans conformation is 6°, compared to 30° in a cis bond, resulting in trans bonds having a more extended conformation allowing for denser packing and reduced membrane fluidity [45]. The conversion of cis to trans is a known response of bacteria to temperature and solvent stress [46,47]. Trans unsaturated bonds appear to convey resistance to butanol in liposome models and may be related to tolerance in vivo. It is possible that the presence of trans bonds can somewhat counter act the fluidising effect of butanol on the membrane.

The substitution of 12.5 % (mass) POPE for POPE which contained a plasmalogen also appeared to have an effect on CF leakage. Liposomes containing the plasmalogen species had lower fluorescence at high butanol concentrations (>30 mg/ml). A decrease in plasmalogen containing species was seen in both lipidomics experiments in high butanol environments (Figs. 1 and 4). This is interesting as in *Clostridium pasteurianum* the amount of plasmalogens was also found to correlate with the highest productivity of butanol (exponential phase) [20]. The content of plasmalogens was also then found to reduce compared to this by the end of the fermentation. Molecular dynamic simulations have shown the rigidifying effects of plasmalogen species on membranes when compared to POPC [31]. One would assume therefore, that a reduction in these species during fermentation would be counterproductive, based on the fluidising effects of butanol on the membrane. However, plasmalogens are also thought to be protective against reactive oxygen species (ROS) [48,49]. They are degraded by ROS and thus may provide protection against any ROS generated in ABE fermentation [50]. It may be that the reduction seen in their abundance is due to them being degraded following reactive species stress in fermentation. This is a speculative theory, and more work is required to understand the exact role of plasmalogens in the response to butanol.

In addition to changes in plasmalogen content, increased chain length is seen in Clostridia with butanol or temperature stress [25,51]. There appears to be a relationship between increased membrane rigidity and decreased membrane permeabilisation during butanol exposure. This relationship could be exploited in engineering strategies to lead to more robust and potentially higher producing strains. However, engineering of membrane fluidity in Clostridia may be challenging. The synthesis of unsaturated bonds in Clostridia remains relatively unclear, though is believed that *fabF* plays a role [21,52] making this a potentially difficult engineering target. A synthetic pathway for plasmalogen lipids in *Clostridium perfringens* has recently been discovered [48]. Characterisation of this system in solventogenic Clostridia would be a useful tool for developing a deeper understanding of any protective role of plasmalogens against butanol production. It is possible that the introduction of well-characterised heterologous enzymes that control membrane saturation could form the basis of a successful strategy. Indeed, Tan and colleagues, [14] show that expression of cis-trans isomerase (CTI) from *Pseudomonas putida* in *E. coli* increased membrane rigidity and tolerance of several alcohols and unfavourable industrial conditions. A related modulation to the acyl chains of the fatty acids is methylation of unsaturated bonds by cyclopropane fatty acid synthase (*cfa)* resulting in cyclopropane fatty acids (CFA). The cyclopropanations of unsaturated bonds with CFA may make membranes more stable through promoting higher membrane order by limiting the rotations around the cyclopropane functional group [53]. Patakova and colleagues found *C. beijerinckii cfa* expression to be upregulated during fermentation when butanol was clearly detectable [21], potentially

suggesting a regulatory relationship between butanol and CFA synthase expression. Later work also showed *cfa* to be upregulated 30 min after the addition of butanol [8]. Interestingly, overexpression of *cfa* in *C. acetobutylicum* ATCC 824 lead to increase resistance to butanol, however also appeared to interfere with the induction of solventogenesis [54]. The exact role of CFA in butanol tolerance requires more investigation. Due to the lack of appropriate standards and sufficient fragmentation data the prevalence of CFA could not be determined in for samples in this study. This may require a more targeted lipidomic methodology in order to accurately gauge.

5. Conclusion

Here, we have observed lipidomic changes in the cell membrane of *C. saccharoperbutylacetonicum* N 1–4 (HMT) during butanol fermentation. This suggests that alterations in the PE:PG ratio and membrane fluidity are key in protecting from butanol stress. Complementary in vitro and in silico experiments have revealed that these changes protect against butanol-induced fluidisation and permeabilisation of the membrane and suggest that butanol acts in a detergent-like manner to disrupt membrane integrity. Moreover, this study has highlighted both phospholipid head group composition, and membrane fluidity, as key targets for rational strain improvement for butanol tolerance.

Declaration of competing interest

The authors declare the following financial interests/personal relationships which may be considered as potential competing interests:

Alan Goddard reports financial support was provided by Biotechnology and Biological Sciences Research Council.

Acknowledgements

We are grateful for funding from Aston University (JL PhD Scholarship) and BBSRC (BB/S01943X/1 and BB/R02152X/1 – ADG and ARP).

References

[1] M. Mascal, Chemicals from biobutanol: technologies and markets, Biofuels Bioprod. Biorefin. (2012), https://doi.org/10.1002/bbb.1328.
[2] S. Nanda, D. Golemi-Kotra, J.C. McDermott, A.K. Dalai, I. Gökalp, J.A. Kozinski, Fermentative production of butanol: perspectives on synthetic biology, New Biotechnol. (2017), https://doi.org/10.1016/j.nbt.2017.02.006.
[3] Y.N. Zheng, L.Z. Li, M. Xian, Y.J. Ma, J.M. Yang, X. Xu, D.Z. He, Problems with the microbial production of butanol, J. Ind. Microbiol. Biotechnol. (2009), https://doi.org/10.1007/s10295-009-0609-9.
[4] C.R. Fischer, D. Klein-Marcuschamer, G. Stephanopoulos, Selection and optimization of microbial hosts for biofuels production, Metab. Eng. 10 (2008) 295–304, https://doi.org/10.1016/j.ymben.2008.06.009.
[5] K. Jia, Y. Zhang, Y. Li, Identification and characterization of two functionally unknown genes involved in butanol tolerance of Clostridium acetobutylicum, PLoS One 7 (6) (2012), e38815, https://doi.org/10.1371/journal.pone.0038815.
[6] S.Y. Lee, J.H. Park, S.H. Jang, L.K. Nielsen, J. Kim, K.S. Jung, Fermentative butanol production by clostridia, Biotechnol. Bioeng. 101 (2008) 209–228, https://doi.org/10.1002/bit.22003.
[7] S. Li, L. Huang, C. Ke, Z. Pang, L. Liu, Pathway dissection, regulation, engineering and application: lessons learned from biobutanol production by solventogenic clostridia, Biotechnol. Biofuels 13 (2020) 39, https://doi.org/10.1186/s13068-020-01674-3.
[8] K. Vollherbst Schneck, J.A. Sands, B.S. Montenecourt, Effect of butanol on lipid composition and fluidity of Clostridium acetobutylicum ATCC 824, Appl. Environ. Microbiol. 47 (1984) 193–194.
[9] J. Guo, J.C.S. Ho, H. Chin, A.E. Mark, C. Zhou, S. Kjelleberg, B. Liedberg, A. N. Parikh, N.-J. Cho, J. Hinks, Y. Mu, T. Seviour, Response of microbial membranes to butanol: interdigitation vs. disorder, Phys. Chem. Chem. Phys. 21 (2019) 11903–11915, https://doi.org/10.1039/C9CP01469A.
[10] N.R. Sandoval, E.T. Papoutsakis, Engineering membrane and cell-wall programs for tolerance to toxic chemicals: beyond solo genes, Curr. Opin. Microbiol. (2016), https://doi.org/10.1016/j.mib.2016.06.005.
[11] F. Wang, S. Kashket, E.R. Kashket, Maintenance of ΔpH by a butanol-tolerant mutant of Clostridium beijerinckii, Microbiology 151 (2005) 607–613, https://doi.org/10.1099/mic.0.27587-0.
[12] P.B. Besada-Lombana, R. Fernandez-Moya, J. Fenster, N.A. Da Silva, Engineering Saccharomyces cerevisiae fatty acid composition for increased tolerance to octanoic acid, Biotechnol. Bioeng. 114 (2017) 1531–1538, https://doi.org/10.1002/bit.26288.
[13] H. Yazawa, Y. Kamisaka, K. Kimura, M. Yamaoka, H. Uemura, Efficient accumulation of oleic acid in Saccharomyces cerevisiae caused by expression of rat elongase 2 gene (rELO2) and its contribution to tolerance to alcohols, Appl. Microbiol. Biotechnol. 91 (2011) 1593–1600, https://doi.org/10.1007/s00253-011-3410-4.
[14] Z. Tan, J.M. Yoon, D.R. Nielsen, J.V. Shanks, L.R. Jarboe, Membrane engineering via trans unsaturated fatty acids production improves Escherichia coli robustness and production of biorenewables, Metab. Eng. 35 (2016) 105–113, https://doi.org/10.1016/J.YMBEN.2016.02.004.
[15] S. Nawab, N. Wang, X. Ma, Y. Huo, Genetic engineering of non-native hosts for 1-butanol production and its challenges: a review, Microb. Cell Factories 19 (2020) 79, https://doi.org/10.1186/s12934-020-01337-w.
[16] A.N. Atmadjaja, V. Holby, A.J. Harding, P. Krabben, H.K. Smith, E.R. Jenkinson, CRISPR-Cas, a highly effective tool for genome editing in Clostridium saccharoperbutylacetonicum N1-4(HMT), FEMS Microbiol. Lett. 366 (2019) 59, https://doi.org/10.1093/FEMSLE/FNZ059.
[17] E.G. Bligh, W.J. Dyer, A rapid method of total lipid extraction and purification, Can. J. Biochem. Physiol. 37 (1959) 911–917, https://doi.org/10.1139/o59-099.
[18] J.C.M. Stewart, Colorimetric determination of phospholipids with ammonium ferrothiocyanate, Anal. Biochem. 104 (1980) 10–14, https://doi.org/10.1016/0003-2697(80)90269-9.
[19] W. Humphrey, A. Dalke, K. Schulten, VMD - visual molecular dynamics, J. Mol. Graph. 14 (1996) 33–38.
[20] J. Kolek, P. Patáková, K. Melzoch, K. Sigler, T. Řezanka, Changes in membrane plasmalogens of Clostridium pasteurianum during butanol fermentation as determined by lipidomic analysis, PLoS One 10 (2015), https://doi.org/10.1371/journal.pone.0122058.
[21] P. Patakova, B. Branska, K. Sedlar, M. Vasylkivska, K. Jureckova, J. Kolek, P. Koscova, I. Provaznik, Acidogenesis, solventogenesis, metabolic stress response and life cycle changes in Clostridium beijerinckii NRRL B-598 at the transcriptomic level, Sci. Rep. 9 (2019) 1–21, https://doi.org/10.1038/s41598-018-37679-0.
[22] C.A. Schneider, W.S. Rasband, K.W. Eliceiri, NIH image to ImageJ: 25 years of image analysis, Nat. Methods 9 (2012) (2012) 671–675, https://doi.org/10.1038/nmeth.2089 (7 9).
[23] P. Durre, Handbook of Clostridia, 2005.
[24] S.J. Routledge, J.A. Linney, A.D. Goddard, Liposomes as models for membrane integrity, Biochem. Soc. Trans. 47 (2019), https://doi.org/10.1042/BST20190123.
[25] S.H. Baer, H.P. Blaschek, T.L. Smith, Effect of butanol challenge and temperature on lipid composition and membrane fluidity of butanol-tolerant Clostridium acetobutylicum, Appl. Environ. Microbiol. 53 (1987) 2854–2861.
[26] T. Ezeji, C. Milne, N.D. Price, H.P. Blaschek, Achievements and perspectives to overcome the poor solvent resistance in acetone and butanol-producing microorganisms, Appl. Microbiol. Biotechnol. (2010), https://doi.org/10.1007/s00253-009-2390-0.
[27] S. Huffer, M.E. Clark, J.C. Ning, H.W. Blanch, D.S. Clark, Role of alcohols in growth, lipid composition, and membrane fluidity of yeasts, bacteria, and archaea, Appl. Environ. Microbiol. 77 (2011) 6400–6408, https://doi.org/10.1128/AEM.00694-11.
[28] P. Patakova, J. Kolek, K. Jureckova, B. Branska, K. Sedlar, M. Vasylkivska, I. Provaznik, Deeper below the surface — transcriptional changes in selected genes of Clostridium beijerinckii in response to butanol shock, MicrobiologyOpen 10 (2021) 1–14, https://doi.org/10.1002/mbo3.1146.
[29] K. Murzyn, T. Róg, M. Pasenkiewicz-Gierula, Phosphatidylethanolamine-phosphatidylglycerol Bilayer as a Model of the Inner Bacterial Membrane, 2005, p. 88, https://doi.org/10.1529/biophysj.104.048835.
[30] N.E. Braverman, A.B. Moser, Functions of plasmalogen lipids in health and disease, Biochim. Biophys. Acta Mol. basis Dis. (2012), https://doi.org/10.1016/j.bbadis.2012.05.008.
[31] T. Rog, A. Koivuniemi, The biophysical properties of ethanolamine plasmalogens revealed by atomistic molecular dynamics simulations, Biochim. Biophys. Acta 1858 (2016) 97–103, https://doi.org/10.1016/j.bbamem.2015.10.023.
[32] M. Lairón-Peris, S.J. Routledge, J.A. Linney, J. Alonso-del-Real, C.M. Spickett, A. R. Pitt, J.M. Guillamón, E. Barrio, A.D. Goddard, A. Querol, Lipid composition analysis reveals mechanisms of ethanol tolerance in the model yeast Saccharomyces cerevisiae, Appl. Environ. Microbiol. 87 (2021) 1–22, https://doi.org/10.1128/AEM.00440-21.
[33] H.V. Ly, M.L. Longo, The influence of short-chain alcohols on interfacial tension, mechanical properties, area/molecule, and permeability of fluid lipid bilayers, Biophys. J. 87 (2004) 1013–1033, https://doi.org/10.1529/biophysj.103.034280.
[34] M. Kanno, T. Katayama, H. Tamaki, Y. Mitani, X.-Y. Meng, T. Hori, T. Narihiro, N. Morita, T. Hoshino, I. Yumoto, N. Kimura, S. Hanada, Y. Kamagata, Isolation of butanol- and isobutanol-tolerant bacteria and physiological characterization of their butanol tolerance, Appl. Environ. Microbiol. 79 (2013) 6998–7005, https://doi.org/10.1128/AEM.02900-13.
[35] D. Lichtenberg, H. Ahyayauch, F.M. Goñi, F. Lix, M. Goñ, The mechanism of detergent solubilization of lipid bilayers, Biophys. Soc. (2013), https://doi.org/10.1016/j.bpj.2013.06.007.
[36] S.M. Smith, Strategies for the purification of membrane proteins, in: Methods in Molecular Biology (Clifton, N.J.), 2017, pp. 389–400, https://doi.org/10.1007/978-1-4939-6412-3_21.
[37] M. Pasenkiewicz-Gierula, K. Baczynski, M. Markiewicz, K. Murzyn, Computer modelling studies of the bilayer/water interface, Biochim. Biophys. Acta Biomembr. 1858 (2016) 2305–2321, https://doi.org/10.1016/J.BBAMEM.2016.01.024.

[38] E. Yamamoto, T. Akimoto, M. Yasui, K. Yasuoka, Origin of subdiffusion of water molecules on cell membrane surfaces, Sci. Rep. 4 (2015) 4720, https://doi.org/10.1038/srep04720.
[39] W. Zhao, T. Róg, A.A. Gurtovenko, I. Vattulainen, M. Karttunen, Role of phosphatidylglycerols in the stability of bacterial membranes, Biochimie 90 (6) (2008) 930–938, https://doi.org/10.1016/j.biochi.2008.02.025.
[40] J.T.J. Cheng, J.D. Hale, M. Elliott, R.E.W. Hancock, S.K. Straus, The importance of bacterial membrane composition in the structure and function of aurein 2.2 and selected variants, Biochim. Biophys. Acta Biomembr. 1808 (2011) 622–633, https://doi.org/10.1016/J.BBAMEM.2010.11.025.
[41] F.J. Weber, J.A.M. de Bont, Adaptation mechanisms of microorganisms to the toxic effects of organic solvents on membranes, Biochim. Biophys. Acta Rev. Biomembr. 1286 (1996) 225–245, https://doi.org/10.1016/S0304-4157(96)00010-X.
[42] J.L. Ramos, E. Duque, J.J. Rodríguez-Herva, P. Godoy, A. Haïdour, F. Reyes, A. Fernández-Barrero, Mechanisms for solvent tolerance in bacteria, J. Biol. Chem. 272 (1997) 3887–3890, https://doi.org/10.1074/jbc.272.7.3887.
[43] Z. Tan, P. Khakbaz, Y. Chen, J. Lombardo, J.M. Yoon, J.V. Shanks, J.B. Klauda, L. R. Jarboe, Engineering Escherichia coli membrane phospholipid head distribution improves tolerance and production of biorenewables, Metab. Eng. 44 (2017) 1–12, https://doi.org/10.1016/j.ymben.2017.08.006.
[44] T. Denich, L. Beaudette, H. Lee, J. Trevors, Effect of selected environmental and physico-chemical factors on bacterial cytoplasmic membranes, J. Microbiol. Methods 52 (2003) 149–182, https://doi.org/10.1016/S0167-7012(02)00155-0.
[45] T. Róg, K. Murzyn, R. Gurbiel, Y. Takaoka, A. Kusumi, M. Pasenkiewicz-Gierula, Effects of phospholipid unsaturation on the bilayer nonpolar region: a molecular simulation study, J. Lipid Res. 45 (2004) 326–336, https://doi.org/10.1194/jlr.M300187-JLR200.
[46] H.J. Heipieper, G. Neumann, S. Cornelissen, F. Meinhardt, Solvent-tolerant bacteria for biotransformations in two-phase fermentation systems, Appl. Microbiol. Biotechnol. 74 (2007) 961–973, https://doi.org/10.1007/s00253-006-0833-4.
[47] H. Okuyama, N. Okajima, S. Sasaki, S. Higashi, N. Murata, The cis/trans isomerization of the double bond of a fatty acid as a strategy for adaptation to changes in ambient temperature in the psychrophilic bacterium, Vibrio sp. strain ABE-1, Biochim. Biophys. Acta, Lipids Lipid Metab. 1084 (1991) 13–20, https://doi.org/10.1016/0005-2760(91)90049-N.
[48] D.R. Jackson, C.D. Cassilly, D.R. Plichta, H. Vlamakis, H. Liu, S.B. Melville, R. J. Xavier, J. Clardy, Plasmalogen biosynthesis by anaerobic bacteria: identification of a two-gene operon responsible for plasmalogen production in Clostridium perfringens, ACS Chem. Biol. 16 (2021) 6–13, https://doi.org/10.1021/ACSCHEMBIO.0C00673.
[49] T. Řezanka, Z. Křesinová, I. Kolouchová, K. Sigler, Lipidomic analysis of bacterial plasmalogens, Folia Microbiol. 57 (2012) 463–472, https://doi.org/10.1007/s12223-012-0178-6.
[50] Z.Y. Liu, X.Q. Yao, Q. Zhang, Z. Liu, Z.J. Wang, Y.Y. Zhang, F.L. Li, Modulation of the acetone/butanol ratio during fermentation of corn stover-derived hydrolysate by Clostridium beijerinckii strain NCIMB 8052, Appl. Environ. Microbiol. 83 (2017), https://doi.org/10.1128/AEM.03386-16.
[51] K.P. Venkataramanan, Y. Kurniawan, J.J. Boatman, C.H. Haynes, K.A. Taconi, L. Martin, G.D. Bothun, C. Scholz, Homeoviscous response of Clostridium pasteurianum to butanol toxicity during glycerol fermentation, J. Biotechnol. 179 (2014) 8–14, https://doi.org/10.1016/J.JBIOTEC.2014.03.017.
[52] L. Zhu, J. Cheng, B. Luo, S. Feng, J. Lin, S. Wang, J.E. Cronan, H. Wang, Functions of the Clostridium acetobutylicium FabF and FabZ proteins in unsaturated fatty acid biosynthesis, BMC Microbiol. 9 (2009) 119, https://doi.org/10.1186/1471-2180-9-119.
[53] D. Poger, A.E. Mark, A ring to rule them all: the effect of cyclopropane fatty acids on the fluidity of lipid bilayers, J. Phys. Chem. B 119 (17) (2015) 5487–5495, https://doi.org/10.1021/acs.jpcb.5b00958.
[54] Y. Zhao, L.A. Hindorff, A. Chuang, M. Monroe-Augustus, M. Lyristis, M.L. Harrison, F.B. Rudolph, G.N. Bennett, Expression of a cloned cyclopropane fatty acid synthase gene reduces solvent formation in *Clostridium acetobutylicum* ATCC 824, Appl. Environ. Microbiol. 69 (5) (2003) 2831–2841, https://doi.org/10.1128/AEM.69.5.2831-2841.2003.